A Molecular Docking Strategy Identifies Eosin B as a Non-active Site Inhibitor of Protozoal Bifunctional Thymidylate Synthase-Dihydrofolate Reductase*

Chloé E. Atreya‡§, Eric F. Johnson‡¶, John J. Irwin‖, Antonia Dow‡, Kristen M. Massimine‡**‡‡, Isabelle Coppens**, Valeska Stempliuk§§, Stephen Beverley§§, Keith A. Joiner**, Brian K. Shoichet‖, and Karen S. Anderson‡¶¶

*From the ‡Department of Pharmacology and the **Infectious Diseases Section, Department of Internal Medicine, Yale University School of Medicine, New Haven, Connecticut 06520, the ‖Department of Molecular Pharmacology and Biological Chemistry, Northwestern University, Chicago, Illinois 60611, and the §§Department of Molecular Microbiology, Washington University School of Medicine, St. Louis, Missouri 63110*

Protozoal parasites are unusual in that their thymidylate synthase (TS) and dihydrofolate reductase (DHFR) enzymes exist on a single polypeptide. In an effort to probe the possibility of substrate channeling between the TS and DHFR active sites and to identify inhibitors specific for bifunctional TS-DHFR, we used molecular docking to screen for inhibitors targeting the shallow groove connecting the two active sites. Eosin B is a 100 μM non-active site inhibitor of *Leishmania major* TS-DHFR identified by molecular docking. Eosin B slows both the TS and DHFR reaction rates. When Arg-283, a key residue to which eosin B is predicted to bind, is mutated to glutamate, however, eosin B only minimally inhibits the TS-DHFR reaction. Additionally, eosin B was found to be a 180 μM inhibitor of *Toxoplasma gondii* in both biochemical and cell culture assays.

Electrostatic channeling is a mechanism proposed based on the crystal structure of bifunctional thymidylate synthase-dihydrofolate reductase (TS-DHFR)[1] from *Leishmania major* that would enable negatively charged dihydrofolate produced at the TS active site to be handed-off along a series of solvent-exposed lysine and arginine residues to the DHFR active site, where it is converted to tetrahydrofolate (1).

In protozoal parasites, the enzymes TS and DHFR exist as a bifunctional enzyme on a single polypeptide chain. The crystal structure of *L. major* TS-DHFR revealed a shallow, basic residue-rich groove connecting the two enzyme active sites (1). Based on this structural finding, it has been proposed that the negatively charged dihydrofolate (H₂folate) produced at the TS active site is electrostatically channeled to the DHFR active site, where it is converted to tetrahydrofolate (H₄folate) without equilibration in bulk solvent (1, 2). The shallow groove region is unique to bifunctional TS-DHFR enzymes; however, how channeling occurs and its physiological significance has not been completely established. We used two concurrent approaches to address this issue: the first being mutagenesis of solvent-exposed basic residues thought to play key roles if the channeling behavior is electrostatic in nature.[2] Our second approach, presented here, is to attempt to physically obstruct channeling and/or domain-domain communication. In the case of tryptophan synthase, where substrate channeling occurs through a hydrophobic tunnel, mutation alone was sufficient to obstruct channeling (4). With TS-DHFR our approach was to identify small molecules that may bind in various areas within the shallow electrostatic groove and to examine their ability to inhibit enzymatic activity as well as parasite growth in cell culture.

In an effort to discover an inhibitor that would bind in the unique shallow groove region of the bifunctional TS-DHFR enzyme, we turned to molecular docking screens of the Available Chemicals Directory (ACD) data base. Such a strategy has been previously used to discover novel inhibitors of monofunctional TS, where a competitive inhibitor found by screening with the program NWU DOCK (5–7) was used as a novel scaffold compound for in-parallel, solid-phase synthetic elaboration, generating an analog with a K_i of 1.3 μM (8). In addition, a preliminary DOCK screen produced a 900 μM non-competitive TS active-site inhibitor: a subsequent similarity search yielded derivatives with K_i values of less than 10 μM (9). More broadly, both monofunctional TS and DHFR enzymes have been the foci of intense structure-based design efforts and are considered model enzymes for such projects (10–12).

An unusual aspect of this project was the targeting of sites in the bifunctional TS-DHFR enzyme located in regions remote from the active sites. Enzyme active sites have traditionally served as the basis of structure-based drug discovery because they represent well defined and highly functionalized targets. By contrast, the shallow groove connecting the TS and DHFR active sites in bifunctional enzymes presents a particular

[1] The abbreviations used are: TS-DHFR, thymidylate synthase-dihydrofolate reductase bifunctional enzyme (this is a functional designation as dihydrofolate is produced at TS and used at DHFR. Elsewhere the bifunctional enzyme is referred to as DHFR-TS because DHFR resides at the N-terminal portion of the bifunctional protein); TS, thymidylate synthase; DHFR, dihydrofolate reductase; dUMP, 2-deoxyuridate; CH₂H₄folate, methylene tetrahydrofolate; H₂folate, dihydrofolate; H₄folate, tetrahydrofolate; ACD, Available Chemicals Directory; HPLC, high performance liquid chromatography.

[2] C. E. Atreya, E. F. Johnson, J. Williamson, S-Y. Chang, P-H. Liang, and K. S. Anderson, unpublished data.

FIG. 1. **Binding site of eosin B as predicted by DOCK.** Target areas for DOCK searches in the putative electrostatic channel region of *L. major* TS-DHFR with eosin B bound (*A*). The shallow groove with the eosin B ligand shown in its best-docked orientation with carbon atoms in *green* (*structure inset*). The DHFR- and TS-binding sites are labeled, and the crystallographic ligands are displayed with carbon colored *cyan*. Stereo pair of the orientation of eosin B in the *L. major* TS-DHFR crystal structure as predicted by DOCK (*B*). Close polar contacts are indicated with *dotted lines* and the distance shown in Angstroms. Key residues are labeled: Arg-283, Glu-151, and the backbone carbonyl of Val-505 make close polar contacts with the ligand. Trp-286, Tyr-508, and Val-505 form a hydrophobic pocket for the phenyl moiety of eosin B.
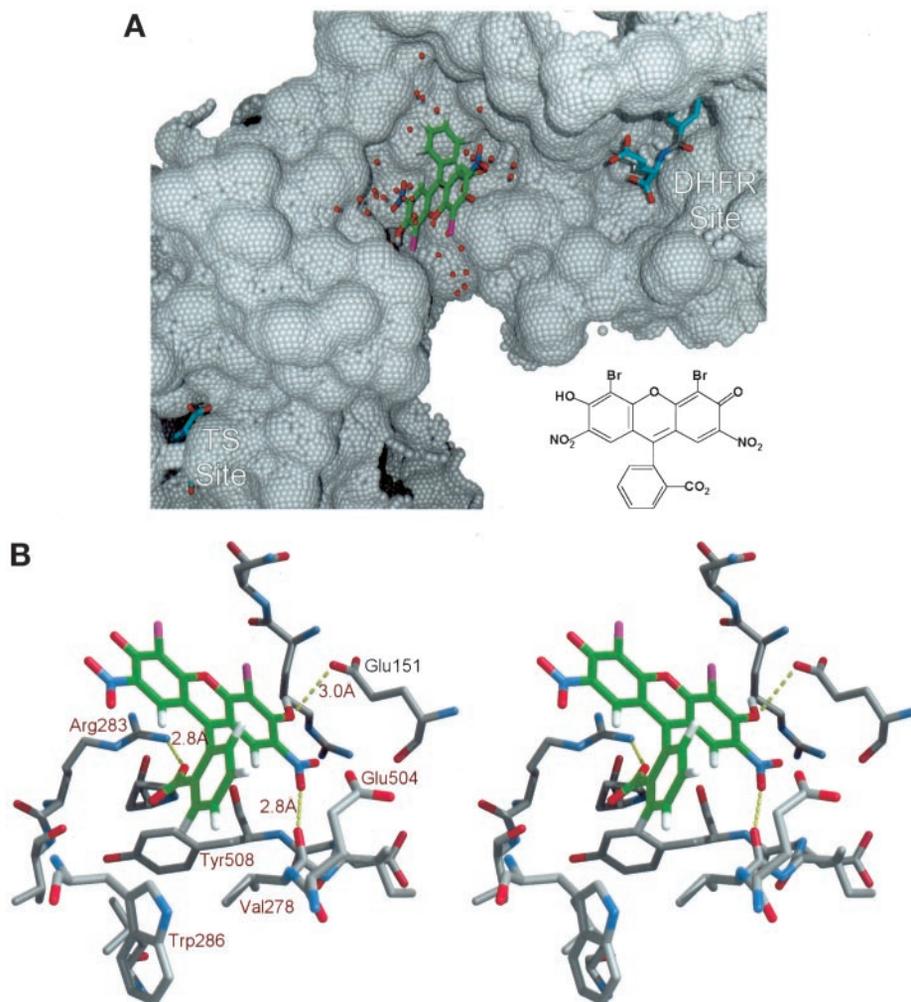
challenge to structure-based efforts, including molecular docking. Successful targeting of the shallow groove region connecting the two active sites and forming the putative channel could produce novel and more specific therapies for protozoal diseases including toxoplasmosis and drug-resistant malaria.

Several docking searches were performed against subregions of a surface area of ~20 × 25 Å thought to define the central region of the electrostatic channel in *L. major* TS-DHFR (Fig. 1*A*). This area includes the basic residues Lys-66, -67, -72, -73, -282 and Arg-64, -283, and -287, believed to be involved in shuttling the intermediate substrate, dihydrofolate, between the two catalytic sites (1). Four subregions of the putative channel were screened against the 152,571 compounds in the 1995.2 version of the ACD of commercially available chemicals. From these screens, 14 compounds were purchased for testing as inhibitors of TS-DHFR (Table I).

We report here that eosin B, predicted by DOCK to bind in the shallow groove region of the putative channel including Arg-283 in the TS domain and Glu-151 in the DHFR domain (Fig. 1*B*), inhibits the bifunctional enzyme. Eosin B (4'-5'-dibromo-2'7'-dinitrofluorescein) is a halogenated xanthene dye (see Fig. 1*A* and Table I) whose spectrophotometric properties have been taken advantage of to measure the protein concentration at low pH (1–3) (13). Whereas related halogenated fluorescein derivatives are thought to be nonspecific inhibitors of several enzymes, acting through an aggregation-based mechanism, extensive kinetic characterization suggests that eosin B is inhibiting the bifunctional enzyme specifically (14).

EXPERIMENTAL PROCEDURES
Computational Work

All docking calculations were performed with the December 1999 development version of NWU DOCK, a version derived from UCSF DOCK 3.5. This version incorporates the ensemble method of ligand flexibility for up to 2000 conformations per molecule (5). The polar and non-polar close contact limits used in the steric grids were 2.3 and 2.6 Å (15). The AMBER united atom charge set, distributed with Delphi, was used for all receptor electrostatic calculations. CHEMGRID was used to calculate a van der Waals potential for the enzyme using standard potentials (16). Chemical labeling was used (17) in the matching calculation. This involves labeling site positions or atoms by chemical properties to speed the docking calculation. Here, five labels were employed: positive, negative, hydrogen bond donor, hydrogen bond acceptor, and neutral. All water molecules and counterions were removed from the receptor model.

We used the *L. major* TS-DHFR coordinates provided to us by Dr. David Matthews (1). A dielectric of 2 for the protein interior (18) and 78 (19) for the water phase were used in the DelPhi calculations. The internal and external dielectrics in the hydration calculation were also set to 2 and 78. In the DelPhi calculation the probe size was set to 1.4 Å. Atomic van der Waals radii for the protein and the ligand were taken from Rashin (19). In the Delphi calculation, the ionic exclusion radius was set to 2 Å and the ionic molarity was set to 0.1 M. The proper values of ligand and protein dielectrics, probe, van der Waals, and ionic radii are active areas of research; we have not tried to optimize these terms. In the receptor potential calculation, three-step focusing (20) was used with protein containment iteratively set to 20, 60, and 90% with a 65.3 A3 lattice.

All data base searches used the same 152,571 molecule subset of the 1995.2 release of the ACD (21). These molecules were selected based on our ability to calculate partial atomic charges (16) and included most of the molecules in the ACD-3D. Partial atomic charges were calculated by

the method of Gasteiger and Marsili (22). Ligand solvation corrections were calculated using HYDREN (15).

The shallow groove region between the TS and DHFR-binding sites was explored using sets of spheres to describe the channel. Spheres were prepared starting from the sphgen program and filtered through the cluster program (16, 23), and then edited by hand using Midas (24). 37 receptor spheres were used. The mean number of orientations per molecule was 3000. Eosin B, ACD code MFCD00005041, scored −14.2 kcal/mol in run 7, placing its rank as 198 of 152,571 molecules. The best energy score in the same run was −37 kcal/mol.

Chemicals

All buffers and other reagents employed were of the highest chemical purity. Millipore ultrapure water was used for all solutions. CH_2H_4folate and H_2folate were purchased from Schircks Laboratories (Switzerland). H_4folate was synthesized by reduction of folic acid with sodium borohydride. Tritium-labeled H_2folate and CH_2H_4folate were synthesized using tritiated folic acid as a starting material: [3′,5′,7,9-^{3}H]folic acid was obtained from Moravek Biochemicals (Brea, CA). Tritium-labeled H_2folate was chemically prepared from the reduction of folate by sodium hydrosulfite (25). Tritiated CH_2H_4folate was prepared enzymatically: tritium-labeled H_2folate was converted to tritiated H_4folate by *L. major* TS-DHFR + NADPH (DHFR reaction), and condensed with formaldehyde to form CH_2H_4folate. The natural (6*R*)-L-CH_2H_4folate enantiomer was purified by DE-52 anion exchange chromatography (Whatman) and used exclusively in the studies. H_2folate and CH_2H_4folate solutions were stored in argon-purged vials at −80 °C. NADPH and dUMP were purchased from Sigma; the concentration of NADPH was determined by using a molar extinction coefficient of 6220 M^{-1} cm^{-1} at 340 nm. Eosin B was purchased from ABCR (A Better Choice for Research Chemicals, Karlsruhe, Germany); fluorescein and phenolphthalein were purchased from Sigma.

Enzymology

The clone of the wild-type bifunctional TS-DHFR enzyme from *L. major* was a generous gift from C.-C. Kan and D. Matthews, then at Agouron Pharmaceuticals. This clone, harboring the pO2CLSA-4 plasmid in an *Escherichia coli* Rue 10 expression vector, was used to obtain protein of high purity (>99%) using previously described methods for purification (26). The wild-type protein has both thymidylate synthase and dihydrofolate reductase activities similar to those previously reported (26–28). The R283E mutation was made using a QuikChange mutagenesis kit (Stratagene). A plasmid containing the desired mutation, as confirmed by nucleic acid sequencing, was used to transform competent BL21. We are grateful to David Roos for the *Toxoplasma gondii* TS-DHFR clone; to Sydney Hoeltzli and Carl Frieden for an *E. coli* DHFR clone; to Louise Wallace and Bob Matthews for *E. coli* DHFR protein; and to Frank Maley for *E. coli* TS protein.

Enzyme Concentrations and Activity Assays

The TS-DHFR protein concentration was estimated spectrophotometrically at 280 nm by using an extinction coefficient of 67,800 M^{-1} cm^{-1} for *L. major* and 78,800 M^{-1} cm^{-1} for *T. gondii* TS-DHFR. The DHFR activity was determined by following the decrease in absorbance at 340 nm that accompanies the conversion of substrates NADPH and H_2folate to products $NADP^+$ and H_4F ($= -12.8$ mM^{-1} cm^{-1}) as described previously. The TS activity was monitored by following the increase in absorbance at 340 nm that accompanies the conversion of substrates dUMP and CH_2H_4folate to dTMP and H_2folate ($=6.4$ mM^{-1} cm^{-1}) (4).

Steady-state Experiments

The reactions were initiated by mixing the 15-μl enzyme solution (0.1–1 μM enzyme; 2× reaction buffer: 1 mM EDTA, 50 mM $MgCl_2$, 50 mM Tris, pH 7.8; saturating NADPH and dUMP; and eosin B in Me_2SO or Me_2SO alone as control) with the 15 μl of CH_2H_4folate. 4% of the final reaction volume was reserved for eosin (1 mM eosin B, final) or Me_2SO (control). The enzyme solution was reacted with 15 μl of substrate: 100–200 μM tritiated CH_2H_4folate (~20,000 dpm). In all cases, concentrations of enzyme and substrates cited in the text are those after mixing. The reactions were terminated by quenching with 67 μl of 0.78 N KOH to give a final concentration of 0.54 N KOH (2).

Rapid Chemical Quench Experiments

The rapid chemical quench experiments were performed using a Kintek RFQ-3 rapid chemical quench apparatus (Kintek Instruments, Austin, TX). Fresh stocks of 25 mM eosin B in Me_2SO were made prior

to each experiment. The final reaction volume was 30 μl; 4% of this was reserved for eosin B (1 mM eosin B, final) or Me_2SO (control). The single enzyme turnover reaction was initiated by mixing the 15 μl of enzyme solution (enzyme + 2× reaction buffer) with the tritiated substrates (15 μl, approximately 20,000 dpm); in all cases, concentrations of enzyme and substrates cited in the text are those after mixing. The TS-DHFR single enzyme turnover reaction was monitored by addition of tritiated CH_2H_4folate to enzyme + NADPH and dUMP. The DHFR reaction was monitored by addition of tritiated H_2folate to enzyme + NADPH. The enzymatic reactions were terminated by quenching with 67 μl of 0.78 N KOH to give a final concentration of 0.54 N KOH (for more details, see Liang and Anderson (2)). The rate constants for individual single-turnover rapid chemical or burst quench experiments were estimated by fitting the data to a single exponential or burst curve using the curve fitting program, Kaleidagraph.

HPLC Analysis—Tritiated products of the rapid quench experiments were quantified by HPLC (high performance liquid chromatography) in combination with a radioactivity flow detector. The HPLC separation was performed using a BDS Hypersil C18 reverse phase column (250 × 4.6 mm, Keystone Scientific, Bellefonte, PA) with a flow rate of 1 ml/min. An isocratic separation using a solvent system of 10% methanol in 180 mM triethylammonium bicarbonate, pH 8.0, was employed. The elution times were as follows: H_4folate, 9 min; H_2folate, 18 min; CH_2H_4folate, 20 min. The HPLC effluent from the column was mixed with liquid scintillation mixture (Monoflow V, National Diagnostics) at a flow rate of 5 ml/min. Radioactivity was monitored continuously using a Flo-One radioactivity-flow detector (Packard Instrument Co.). The analysis system was automated using a Waters 712B WISP (Milford, MA) autosampler.

T. gondii TS-DHFR Homology Model

A homology model of *T. gondii* TS-DHFR was built using the Swiss Protein Database program in conjunction with the Swiss Model homology modeling link available at the Swiss Protein Database website. The C-terminal 315 amino acids (residues 295–610) and residues 115–166 were modeled using the protein database file for the *L. major* TS-DHFR structure. The N-terminal 52 amino acids were modeled using the protein database file for *Pneumocystis carinii* DHFR, which is the highest homology DHFR relative to the N-terminal portion of the *T. gondii* DHFR domain for which a structure was available.

Evaluation of the Ability of Eosin B to Inhibit T. gondii Replication in Cell Culture

Cell Lines and Culture Conditions—Chinese hamster ovary cells were grown as monolayers at 37 °C in an atmosphere of 5% CO_2 in α-minimum essential medium supplemented with 2 mM L-glutamine and penicillin/streptomycin (100 units/ml per 100 μg/ml).

Parasite Cultivation—The RH strain tachyzoite of *T. gondii* was used and maintained by *in vitro* culture in human foreskin fibroblast cells as described previously (29).

Determination of Parasite Viability—Chinese hamster ovary cells were seeded in triplicate at a density of 2×10^4 cells/ml in a 24-well plate, allowed to attach for 24 h, and then infected with *T. gondii*. Parasite cultures were synchronized by removal of parasites that had not yet invaded 4 h after their inoculation into confluent cells. After incubation with various concentrations of eosin B for 24 h, *T. gondii* viability was evaluated 24 h postinfection by measurement of [^{3}H]uracil incorporated into the parasite nucleic acids. Briefly, 1 μCi of radiolabel was added to each well for 2 h before the monolayers were fixed with trichloroacetic acid, rinsed, and counted as described (30).

RESULTS

Molecular Docking Against TS-DHFR—The program NWU-DOCK (5–7), a derivative of DOCK 3.5 (16, 23) was used to screen 152,571 compounds of the ACD 1995.2 data base for molecules complementary to the shallow groove, putative channeling region of protozoal TS-DHFR. To prepare the site for docking, all water and ion molecules were removed. Protonation of receptor residues and water molecules was done with Sybyl (Tripos, St. Louis, MO). Positions of some protons were then rotated manually to more appropriate orientations using MidasPlus (24). The sphere set used contained 57 spheres and was obtained from reclustering spheres obtained from the sphgen program, part of the DOCK 3.5 package (17). Force field and electrostatic grids were calculated with CHEMGRID (16)

TABLE I
DOCK hits tested

The 14 DOCK hits tested, along with the ACD code, two-dimensional structure, and DOCK energy score of each. All inhibitors were tested by rapid chemical quench at a concentration of 1 mM; 50 μM *L. major* TS-DHFR using the same set of reaction conditions as detailed for eosin B. An "*" indicates that upon initial characterization, inhibition was observed at a drug concentration of 1 mM, as compared with a Me$_2$SO control. One compound, 2,5,7-trinitro-9-oxo-9*H*-fluorene-4-carboxylic acid, elicited complex kinetic behavior, appearing to inhibit in a time-dependent and NADPH-dependent manner. Also included in the table are the structures of two subsequently tested eosin B analogs, fluorescein and phenolphthalein.

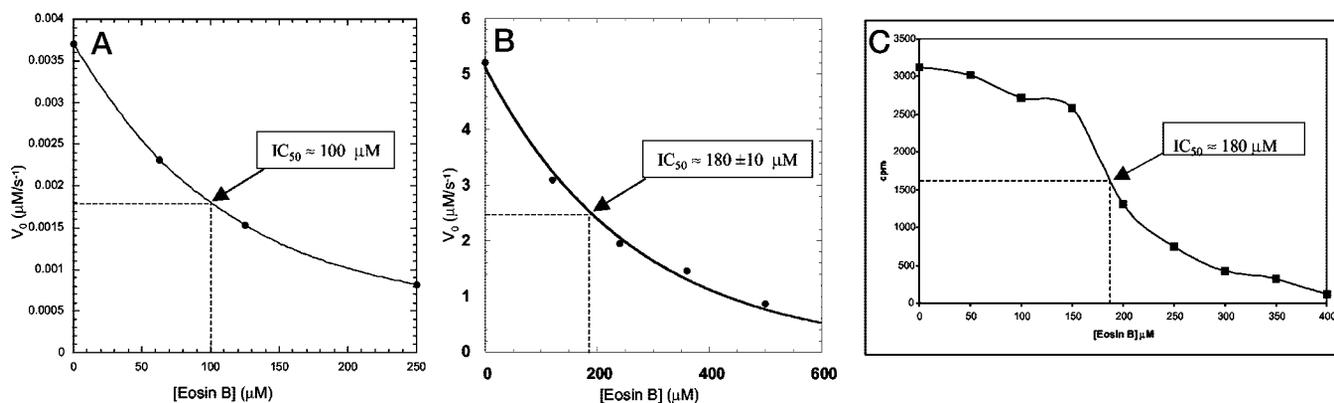| Compound Name/ Chemical Formula/ ACD Code	Structure	DOCK Score (kcal/mol)
Methyl 2-[(3,3-dimethyl-2-oxobutyl)thio]-6-methyl-5,5-dioxo-5,6-dihydro-5-lambda-6-benzo[C]pyrimido[4,5-E][1,2]thiazine-8-carboxylate C$_{19}$H$_{21}$N$_3$O$_5$S$_2$ MFCD00098670		-17.1
2,5,7-trinitro-9-oxo-9H-fluorene-4-carboxylic acid C$_{14}$H$_5$N$_3$O$_9$ MFCD00180008		-14.7 (*)
N-(4-Nitrophenylsulfonyl)-L-phenylalanine C$_{15}$H$_{14}$N$_2$O$_6$S MFCD00191470		-15.7
METHYL 7-FLUORO-2-(METHOXYMETHYL)-5-OXO-5H-CHROMENO[2,3-B]PYRIDINE-3-CARBOXYLATE C$_{16}$H$_{12}$F N O$_5$ MFCD00139064		-16.1
5-ISATINSULFONIC ACID, SODIUM SALT HYDRATE C$_8$H$_4$NO$_5$S •Na •H$_2$O MFCD00192236		-13.1
2,2-dimethyl-4-oxo-7-[(phenylsulfonyl)oxy]-3,4-dihydro-2H-chromen-5-yl-benzene-1-sulfonate C$_{23}$H$_{20}$O$_8$S$_2$ MFCD00205533		-18.7
4-hydroxy-3,5-dinitrobenzoic acid C$_7$H$_4$N$_2$O$_7$ MFCD00017000		-13.7
N-O-NPS-glutamine C$_{11}$H$_{13}$N$_3$O$_5$S MFCD00038157		-15.3
3-amino-3-(2-nitrophenyl)propionic acid C$_9$H$_{10}$N$_2$O$_4$ MFCD00090356		-17.3
2-([4-[(4-bromophenyl)thio]-3-nitrobenzyl]amino)propanoic acid C$_{16}$H$_{15}$Br N$_2$O$_4$S MFCD00205447		-17.4
N3-{4-chloro-2-[(2-phenylhydrazino)carbonyl]phenyl}-2 phenoxynicotinamide C$_{25}$H$_{19}$ClN$_4$O$_3$ MFCD00206034		-24.8
2-(methoxycarbonyl)benzo[b]thiophen-3-yl-2-phenoxynicotinate C$_{22}$H$_{15}$NO$_5$S MFCD00116956		-19.6
5-benzyloxy-DL-tryptophan C$_{18}$H$_{18}$N$_2$O$_3$ MFCD00037968		-12.2
Eosin B C$_{20}$H$_6$Br$_2$N$_2$O$_9$ •2 Na MFCD00005041		-14.2
Fluorescein C20 H12 O5 MFCD00005050		
Phenolphthalein C$_{20}$H$_{14}$O$_4$ MFCD00005913		

Molecular Docking Identifies a TS-DHFR Inhibitor: Eosin B

FIG. 2. **Eosin B dose response.** *A*, steady-state time courses were completed in the presence of 0.1 μM *L. major* TS-DHFR, 200 μM CH$_2$H$_4$folate, and 0 μM (Me$_2$SO control), 62.5, 125, or 250 μM eosin B. An IC$_{50}$ value of 100 μM was obtained by plotting the rates of the steady-state reactions *versus* eosin B concentration. *B*, steady-state time courses with 1.5 μM *T. gondii* TS-DHFR, 500 μM CH$_2$H$_4$folate, and varying concentrations of eosin B yielded an IC$_{50}$ of 180 μM. *C*, in cell culture assays, an eosin B concentration of 180 μM also reduced *T. gondii* replication inside host cells by 50%, as expressed by counts/min of radiolabel incorporated into parasites.

and DelPhi (20), respectively. DISTMAP was used to calculate the excluded volume grid (31).

On average, 3000 orientations and up to 2000 conformations were calculated in the site for each data base molecule. Molecules were scored and ranked based on their van der Waals and electrostatic complementarity to the putative channeling region, and corrected for polar and non-polar desolvation effects (6). The docking calculation took 23 h on an Intel Pentium III 450 MHz CPU. 400 high scoring compounds were visually evaluated in the site in their docked conformations. Based on observed complementarity, and with an eye for testing different scaffolds, 14 compounds were ultimately ordered and tested for inhibition of TS-DHFR (Table I). Of these, one (eosin B) showed significant enzyme inhibition when tested at micromolar concentrations (below).

Steady-state Kinetic Analysis—A preliminary steady-state screening of DOCK hits indicated that eosin B inhibits the bifunctional TS-DHFR reaction, in which CH$_2$H$_4$folate is converted to H$_4$folate. Steady-state time courses for the reaction of 0.1 μM *L. major* TS-DHFR with 200 μM CH$_2$H$_4$folate in the presence of 0, 62, 125, or 250 μM eosin B revealed an IC$_{50}$ of 100 μM (Fig. 2*A*). To evaluate whether the inhibitory activity of eosin B would translate to a similar bifunctional enzyme, the TS-DHFR from *T. gondii* was examined. Steady-state time courses for the reaction of 1.5 μM *T. gondii* TS-DHFR with 500 μM CH$_2$H$_4$folate in the presence of varying concentrations of eosin B yielded an IC$_{50}$ of 180 μM (Fig. 2*B*). In each case, steady-state inhibition by eosin B is saturable; at high eosin B concentrations complete inhibition is achieved.

In steady-state experiments where either 0.1 or 1 μM *L. major* TS-DHFR was reacted with 100 μM CH$_2$H$_4$folate in the presence or absence of 125 μM eosin B, ~50% inhibition was observed at both enzyme concentrations (data not shown). These data indicate that the enzyme inhibition is not dependent on enzyme concentration.

Transient Kinetic Analysis—Transient kinetic analysis was used to obtain a more detailed characterization of the action of eosin, including effects on the single enzyme turnover rates of the TS and DHFR reactions individually, as well as in the bifunctional TS-DHFR reaction, and to look for a build-up of dihydrofolate that may suggest evidence of impaired channeling. Whereas steady-state kinetic analysis is an indirect method from which one can infer information about the rate-limiting step of an enzymatic reaction, transient kinetics allows one to directly measure individual steps in a kinetic pathway as well as to define the reaction kinetics of intermediate formation. Transient kinetics has several advantages for investigation of substrate channeling because, in principle, this technique enables one to directly monitor chemical catalysis at each active site as well as the transit of the putative intermediate from one active site to another (32, 33).

Single enzyme turnover experiments, which measure the rate of the chemical conversion of substrate to product at the active site under conditions where enzyme concentration is sufficiently high that substrate binding is not rate-limiting, were performed using a rapid chemical quench apparatus. For each single enzyme turnover experiment, full time courses for *L. major* in the presence and absence of 1 mM eosin B were completed in duplicate, along with $t = 0$ and $t = 60$ s controls. Because eosin B was dissolved in dimethyl sulfoxide, an equivalent amount of Me$_2$SO (4% of final volume) was added to control reactions. This concentration of Me$_2$SO has no effect on the single-turnover reaction rates (data not shown).

To monitor the DHFR reaction, the bifunctional TS-DHFR enzyme (50 μM) was preincubated with a saturating concentration of NADPH (500 μM) and then mixed with a limiting amount of radiolabeled H$_2$folate (14 or 15 μM). To monitor the TS reaction, the bifunctional TS-DHFR enzyme (50 μM) was preincubated with a saturating concentration of dUMP (500 μM) and then mixed with a limiting amount of radiolabeled CH$_2$H$_4$folate (10 or 12.5 μM). The bifunctional TS-DHFR single enzyme turnover experiment was set up similar to that for TS, except that saturating NADPH (500 μM) was added as well as dUMP. All reported concentrations are final, after mixing.

Eosin B was found to inhibit both the TS and DHFR reactions, but TS was inhibited more strongly (Table II). As predicted, the inhibition of the bifunctional reaction by eosin B is

TABLE II
Species dependence of eosin B inhibition on the TS-DHFR, TS, and DHFR reactions; and effects of eosin B on the L. major R283E mutant

Data are reported as percent activity remaining: rate of the reaction in the presence of 1 mM eosin B divided by the rate with Me$_2$SO alone. All values where an error margin is included represent the average results from 2 to 3 paired time courses. The TS-DHFR reaction is not applicable to the *E. coli* monofunctional enzymes.

Species/enzyme	TS-DHFR	TS	DHFR
L. major	24 ± 3%	23 ± 3%	35 ± 0%
T. gondii	22 ± 3%	29%	28 ± 8%
E. coli	NA[a]	37 ± 0%	91 ± 0%
L. major R283E[b]	80%		30%

[a] Not applicable.

[b] In the case of R283E, 80% of the R283E TS-DHFR activity remains in the presence of 1 mM eosin B, but note that R283E has 40% *L. major* wild-type TS-DHFR activity. R283E has 100% wild-type DHFR activity.
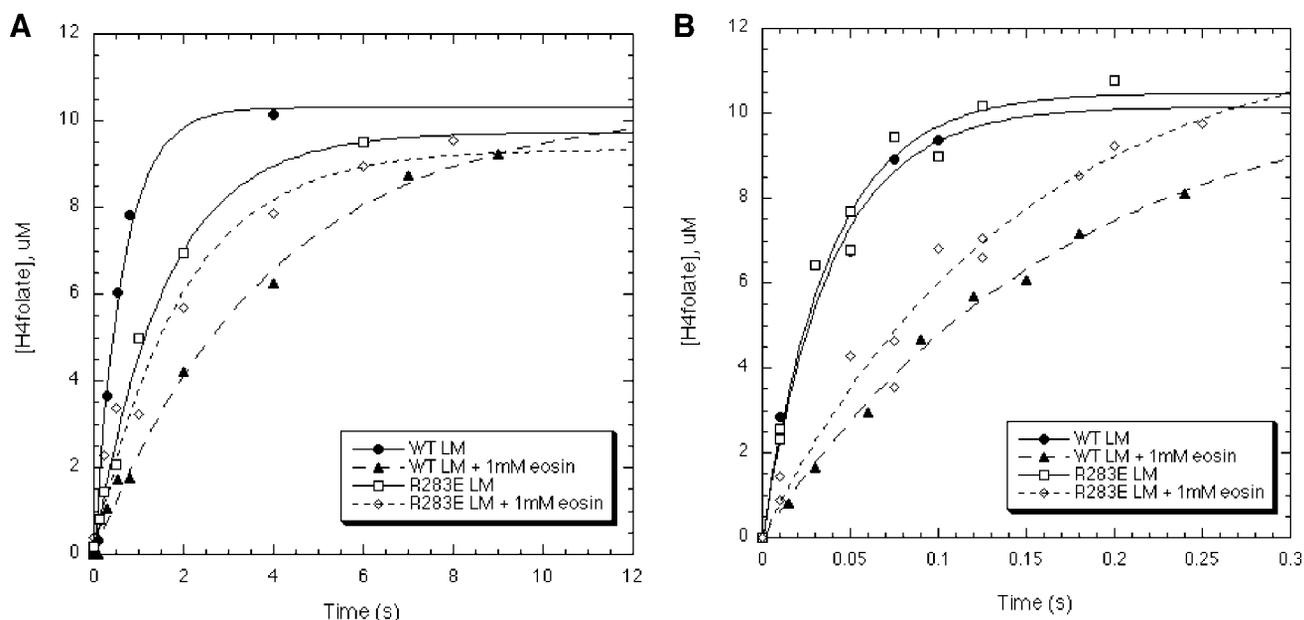
FIG. 3. **Effects of eosin B on the *L. major* R283E mutant TS-DHFR and DHFR reactions.** In the absence of eosin B, R283E has 40% wild-type TS-DHFR activity. The rate of the R283E TS-DHFR reaction is virtually unchanged in the presence of 1 mM eosin B, whereas 1 mM eosin B significantly inhibits the wild-type TS-DHFR reaction (*A*). The R283E DHFR reaction rate is equivalent to that of the wild-type enzyme; 1 mM eosin B reduces the rate of both the R283E and wild-type *L. major* DHFR reactions by ~70% (*B*). All reaction time courses were followed to 60 s, but only early time points are plotted for visual clarity.

equivalent to inhibition of TS alone because the rate of product formation by TS is significantly slower than that of DHFR in *L. major*. The data are presented in Table II as the percent of activity remaining; the ratio of the rate constant obtained in the presence of 1 mM eosin B divided by that with Me$_2$SO alone. In experiments examining the bifunctional TS-DHFR reaction, no dihydrofolate accumulation above background was observed.

To address the question of whether the inhibition observed in the single enzyme turnover experiments described above was because of competition with substrates at the active site, the effect of varying the substrate concentration was examined. When either 3 or 62 μM CH$_2$H$_4$folate was reacted with 250 μM *L. major* TS-DHFR in the presence of 1 mM eosin B, 33–40% activity remained. In the case of the DHFR reaction, equivalent reaction rates were obtained when 4 or 40 μM H$_2$folate was reacted with 100 μM *L. major* TS-DHFR in the presence of 1 mM eosin B. The fact that a 20-fold change in CH$_2$H$_4$folate concentration and a 10-fold change in H$_2$folate concentration had no effect on level of inhibition by eosin B at enzyme concentrations where binding of substrate is not rate-limiting, implies that eosin B binds outside of both the TS and DHFR folate binding pockets.

Species Variations in Inhibition by Eosin B—Because one long-term goal of this research is to develop a therapy specific for protozoal bifunctional TS-DHFR, eosin B was tested against TS-DHFR from an evolutionarily divergent but clinically relevant sporozoan protozoa, *T. gondii*, and against *E. coli* monofunctional TS and DHFR for comparison (Table II). Single turnover experiments were set up as detailed above for *L. major* (50 μM enzyme, 1 mM eosin B or 4% Me$_2$SO, 500 μM dUMP and/or NADPH, with ~10 μM radiolabeled CH$_2$H$_4$folate or H$_2$folate).

The bifunctional TS-DHFR as well as the individual TS and DHFR reactions of *L. major* and *T. gondii* were similarly inhibited by addition of 1 mM eosin B. The *E. coli* TS reaction was slightly less inhibited than that of *L. major*. The striking finding was, however, that whereas ~35% DHFR activity remains with both bifunctional enzymes in the presence of 1 mM eosin B,

E. coli DHFR is almost entirely unaffected by 1 mM eosin B (91% activity remaining). Whereas the TS enzyme is highly conserved across species, the relatively low sequence conservation in DHFR makes sequence alignments inconclusive. Structural alignment of *L. major* with a homology model of *T. gondii* TS-DHFR, however, reveals a similar overall structure in the region of Glu-151, with *T. gondii* residue Asp-146 located very near to and in the same orientation as Glu-151. By contrast, an examination of the aligned crystal structures reveals that the loop structure of *E. coli* in the vicinity of Glu-151 is significantly different from that in *L. major*, and the closest acidic residue, Asp-90, is oriented in a different direction from Glu-151.

Effects of Eosin B on the L. major R283E Mutant—Because eosin B was predicted by the docking program to interact with Arg-283 (R283) in the TS domain of *L. major* TS-DHFR (see Fig. 1*B*), eosin B was tested against the charge reversal mutant, R283E. Whereas mutation of Arg-283 alone produced an enzyme with only 40% of wild-type TS-DHFR activity, addition of 1 mM eosin B only inhibited the mutant enzyme slightly such that >80% activity remains. This sharply contrasts what was seen with the wild-type enzyme where, under the same reaction conditions, 1 mM eosin B strongly inhibits the wild-type enzyme such that ~20% activity remains (Fig. 3*A*). Furthermore, the Arg-283 → Glu substitution had very little effect on ability of eosin to inhibit the DHFR reaction, consistent with the docking prediction (Fig. 3*B*). Effects of eosin B on the *L. major* R283E mutant are summarized in Table II.

Comparative Enzyme Inhibition by Eosin Analogs—To evaluate the contributions of structural components of eosin B to its inhibitory properties, eosin B was compared with 2 analogs: fluorescein and phenolphthalein (see Table I). Fluorescein, the unliganded precursor to eosin B lacking the halogen and nitro groups, was found to be ~8-fold less potent than eosin B itself. At a concentration of 1 mM eosin B, the rate of the TS-DHFR reaction was only 25% that in the absence of inhibitor. In contrast, at 1 mM fluorescein no inhibition was observed; and at 4 mM, a rate that was 50% of the TS-DHFR reaction rate with no inhibitor added could be achieved (Fig. 4).
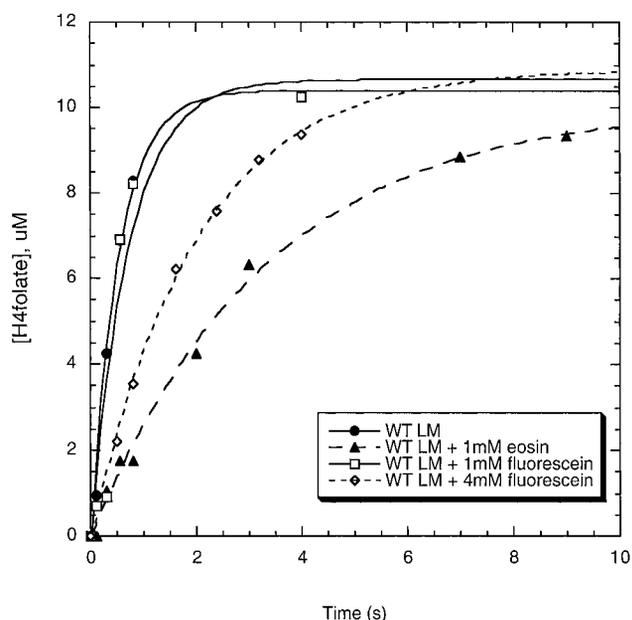
FIG. 4. *L. major* **TS-DHFR inhibition by 1 or 4 mM fluorescein as compared with 1 mM eosin B.** 4 mM fluorescein inhibits wild-type *L. major* approximately half as well as 1 mM eosin B; no inhibition was observed with 1 mM fluorescein.

Phenolphthalein, which also resembles the *cyclic* form of eosin B in that it contains phenolic and benzoic acid moieties (see Table I), has been reported to be a 5 μM TS monofunctional enzyme inhibitor. Structural studies have shown by x-ray crystallography that it binds at the *Lactobacillus casei* TS active site in a region close to but not overlapping with folate binding (9). It is important to note, however, that the docking predictions were made with the *open* tautomer of eosin B and this is also the form favored by our experimental conditions, at neutral pH.

If phenolphthalein is binding at a different site than eosin B, it would not make contact with the conserved Arg residue, so we predicted that it should be just as effective at inhibiting the R283E mutant as the wild-type enzyme. Indeed, unlike eosin B in which sensitivity to inhibition was lost by the R283E mutation, phenolphthalein inhibited this mutant to the same degree as the wild-type enzyme: only 30% of TS-DHFR activity remained when 40 μM phenolphthalein was added to 33 μM R283E (data not shown). No inhibition of DHFR activity was observed under similar conditions.

Parasitology: Effects of Eosin in Cell Culture—The next logical step was to test whether eosin B could affect parasite replication in cell culture. An evaluation of eosin B in kinetoplastid *L. major* parasites revealed it to be a weak (5 mM) inhibitor (data not shown), however, the sensitivity of eosin B was more significant on the apicomplexan parasite, *T. gondii. T. gondii* parasites multiply in a parasitophorous vacuole, whose membrane contains proteinaceous pores (34, 35) that allow the passive bidirectional diffusion of small molecules <1,300, in accord with the molecular weight of eosin B (624,000). It was seen that an eosin B concentration of 180 μM reduces *T. gondii* replication inside host cells by 50%, as measured by [3H]uracil incorporation (Fig. 2*C*); matching the IC$_{50}$ obtained in steady-state biochemical assays (Fig. 2*B*). This is notable because parasite host cells were unaffected up to a drug concentration of 400 μM (assayed by [3H]thymidine incorporation). To establish that the inhibitory effects of eosin B in cell culture were because of effects on the folate pathway, the ability of leucovorin (folinic acid) to "rescue" inhibited cells was assessed. The finding that 10 μM leucovorin reverses the inhi-

bition of replication induced by eosin B provides strong evidence that TS-DHFR is the target of eosin in *T. gondii.*[3]

DISCUSSION

Molecular docking was used to target the shallow groove connecting the TS and DHFR active sites of the *L. major* bifunctional enzyme; the surface originally hypothesized to form an electrostatic channel for the substrate intermediate, dihydrofolate. Eosin B, predicted by NWU DOCK to interact with Arg-283 in the TS domain and Glu-151 in the DHFR domain of the *L. major* bifunctional enzyme, was found to have an IC$_{50}$ value of 100 μM. Although such a level of inhibition is modest by drug standards, first round lead compounds from virtual screening often inhibit in this range; modification can improve these leads by several orders of magnitude (3, 17, 36, 37). Because targeting the non-active site of a molecule for inhibition requires a more in-depth understanding interplay of the mechanism and structure than targeting the active site, we sought to address these issues prior to attempting generation of more potent and specific inhibitors.

A non-active site TS-DHFR inhibitor could act by interfering with channeling of dihydrofolate from TS to DHFR, protein conformational changes constituting TS-DHFR domain-domain communication, or both. As discussed below, a number of experiments did provide evidence that eosin B is a non-active site inhibitor, capable of inhibiting both TS and DHFR. Because the proposed binding site for eosin B is located in the shallow groove region containing the putative electrostatic channel, one might anticipate that a small molecule bound in this region, or mutations that alter charge, might interfere with the transit of dihydrofolate from the TS to the DHFR active site. Accordingly, one might predict that the kinetics would reflect a build-up of the dihydrofolate intermediate in solution. Using a transient kinetic analysis, a single enzyme turnover experiment examining the TS-DHFR reaction did not, however, show a difference in dihydrofolate accumulation in the presence or absence of eosin B. As a likely alternative to inhibition of substrate channeling, eosin B may exert its effect by interfering with domain-domain communication, or the series of protein conformational changes induced by ligand binding at one active site that affects activity at the active site of the other enzyme.

The finding that eosin B only marginally inhibits the *L. major* R283E charge reversal mutant supports the suggestion that eosin B does in fact, interact with Arg-283, a residue located in the shallow groove targeted with the docking program. Whereas phenolphthalein is known by x-ray crystallography to bind to the TS active site, it inhibits R283E to the same degree as wild-type *L. major* TS-DHFR. This observation suggests that the binding sites for eosin B and phenolphthalein are distinct, and is not surprising because phenolphthalein is most similar to the cyclic form of eosin B while the docking predictions and our experimental conditions employ the open form. Nonetheless, the finding indicates that the decreased ability of eosin to bind R283E is unlikely to be because of a remote effect, such as change in the active site conformation, as a result of the non-active site mutation. The fact that TS is a highly conserved enzyme and position 283 is completely conserved as a basic residue (arginine or lysine) across enzyme species could account for the similar TS inhibition observed with the bifunctional and monofunctional enzymes tested.

Conversely, whereas there is high structural similarity between *L. major* and a homology model of *T. gondii* TS-DHFR in

---

the region of Glu-151, limited structural conservation exists with *E. coli* DHFR and the closest acidic residue, Glu-90, is oriented in a different direction from Glu-151; possibly explaining the poor inhibition of eosin in the *E. coli* enzyme. Efforts are underway to definitively elucidate the site of binding of eosin through co-crystallization of eosin B with *L. major* and *T. gondii* TS-DHFR.

Whereas Arg-283 and Glu-151 appear to make key contacts with the hydroxyl groups on eosin B, comparative inhibition by the scaffold molecule, fluorescein, predicts that the hydroxyl groups are not the only functional groups on the molecule that are important for binding. The hydroxyl groups are present on both the scaffold molecule and eosin B, but eosin B is an 8-fold better inhibitor of *L. major* TS-DHFR than is fluorescein. This suggests that the 4′,5′-dibromo and 2′7′-dinitro groups on eosin B also promote binding, either directly or indirectly, by increasing the hydrophobicity of the inhibitor. Reviewing the structure, the one functional group that does not appear to participate in energetically favorable interactions is the 5′ bromine. This bromine does, however, lie close to a hydrophilic pocket near the conserved basic loop in the DHFR domain, and therefore may be ideally positioned for modification. Understanding structural characteristics that contribute to inhibition by eosin B should allow for structure-based design of analogs with greater potency and specificity for the bifunctional enzyme in the future.

The evaluation of the mode of action of eosin using spectroscopic techniques is difficult because, at the concentrations necessary to see inhibition, the dye absorbs light making fluorescence and absorbance studies unfeasible because of inner-filter effects. Transient kinetic studies indicate that eosin B is not competitive with monoglutamyl folate substrates (either CH_2H_4folate or H_2folate). The finding that eosin B inhibits both the TS and DHFR reactions without competing for either folate substrate provides kinetic evidence, supporting the structural predictions of DOCK and results with the R283E mutant, that eosin B binds outside of the active sites of both TS and DHFR.

One aspect of eosin B with which we were concerned was its potential ability to form aggregates in solution that could inhibit many enzymes nonspecifically. Indeed, there is a precedent for fluorinated dyes acting as nonspecific inhibitors (14). Several lines of evidence suggest, however, that eosin B is, in fact, inhibiting *L. major* TS-DHFR specifically. First, IC$_{50}$ values for aggregate-based inhibition are very sensitive to changes in enzyme concentration. With eosin B, on the other hand, steady-state inhibition was unaffected by 10-fold increases in the concentration of *L. major* TS-DHFR (from 0.1 to 1 μM enzyme). If eosin B were forming large aggregates capable of binding up enzyme, the same concentration of aggregates should have been formed in either case, as the same eosin B concentration was used; but a much greater percent inhibition would be observed at low enzyme concentration. Instead ~50% inhibition was seen at both enzyme concentrations. Second, a point substitution, Arg-283 → Glu, diminished the inhibition of eosin by over an order of magnitude, consistent with the docking prediction of a classical 1:1 complex being formed in this region. Finally, in the pre-steady-state kinetics, a ratio of inhibitor:enzyme of 20:1 was used, whereas aggregation-based nonspecific inhibitors appear to require ratios of over 1000:1 (inhibitor:enzyme). Nonspecific inhibition therefore seems unlikely to explain the activity of eosin *versus* TS-DHFR.

Evidence that eosin B is specifically targeting TS-DHFR has been further obtained by cell culture experiments with *T. gondii*. *T. gondii* replication is reduced by 50% at a drug concentration of 180 μM, similar to the IC$_{50}$ of eosin in steady-state biochemical assays with *T. gondii* TS-DHFR protein. Furthermore, growth inhibition induced by eosin B is reduced by administration of leucovorin, a chemical that is used as an antidote to compounds that block the conversion of folic acid to folinic acid.[4] Additionally, concern over potential toxicity related to nonspecific inhibition by eosin B is lessened by the finding that no adverse effects were observed in rats fed diets containing up to 2% eosin B, leading to FDA approval of eosin B for use in drugs and cosmetics.[5]

Differences in folate metabolic pathways as well as drug uptake or stability may account for the poor inhibition of *L. major* by eosin B in cell culture. *L. major* is known to encode P-glycoprotein family members including MDR and MRP homologs, and also contains a large vacuole and acidic compartments not present in other parasites. Eosin B uptake and localization within the various parasites will be a topic of future experimentation.

In principle, non-active site binding regions offer unique opportunities to discover specific inhibitors. Often, however, such sites lack the tightly defined geometrical and functional constraints of active sites and as such are difficult to target. Here we were able to use molecular docking to target the shallow groove region between the TS and DHFR active sites in the *L. major* bifunctional enzyme. Several lines of evidence suggest that eosin B binds outside of the two active sites. The effects of the Arg-283 → Glu point substitution are, moreover, consistent with the docking prediction. Whereas mutation of basic residues in the shallow groove region, including Arg-283, does not appear to affect domain-domain communication, or at least TS catalysis; eosin B binding in this region affects both TS and DHFR activity, presumably by inducing or preventing key conformational changes. This, coupled with the fact that no build-up of dihydrofolate was observed, suggests that eosin B exerts its effects on TS and DHFR via interference with domain-domain communication rather than electrostatic channeling.

Furthermore, comparative inhibition by eosin B analogs has yielded structural information that should allow for design of more potent and specific inhibitors of protozoal TS-DHFR and could produce novel therapies specific for parasitic infections, including toxoplasmosis and malaria, particularly drug-resistant malaria. Eosin B has already been shown to be an inhibitor of *T. gondii* in cell culture at concentrations where host cells are unharmed. As such, findings with eosin B represent an important step toward establishing proof-of-principle that the non-active site, shallow groove region of the bifunctional TS-DHFR enzyme can serve as a molecular target that when inhibited, results in parasite death.

REFERENCES

1. Knighton, D. R., Kan, C-C., Howland, E., Janson, C. A., Hostomska, Z., Welsh, K. M., and Matthews, D. A. (1994) *Nat. Struct. Biol.* **1,** 186–194
2. Liang, P-H., and Anderson, K. S. (1998) *Biochemistry* **37,** 12195–12205
3. Gradler, U., Gerber, H. D., Goodenough-Lashua, D. M., Garcia, G. A., Ficner, R., Reuter, K., Stubbs, M. T., and Klebe, G. (2001) *J. Mol. Biol.* **306,** 455–467
4. Schlichting, I., Yang, X-J., Miles, E. W., Kim, A. Y., and Anderson, K. S. (1994) *J. Biol. Chem.* **43,** 26591–26593
5. Lorber, D. M., and Shoichet, B. K. (1998) *Protein Sci.* **4,** 938–950
6. Shoichet, B. K., Leach, A. R., and Kuntz, I. D. (1999) *Proteins* **34** 4–16
7. Su, A. I., Lorber, D. M., Weston, G. S., Baase, W. A., Matthews, B. W., and

---

[4] Federal Register (1982) *Rules and Regulations 53845*, Vol. 47, No. 230.
[5] National Library of Medicine: www.nlm.nih.gov/medlineplus/druginfo/leucovorinsystemic202321.html.

Shoichet, B. K. (2001) *Proteins* **42,** 279–293
8. Tondi, D., Slomczynka, U., Waterson, D. M., Costi, M. P., and Shoichet, B. K. (1999) *Chem. Biol*. **6,** 319–331
9. Shoichet, B. K., Stroud, R. M., Santi, D. V., Kuntz, I. D., and Perry, K. M. (1993) *Science* **259,** 1445–1450
10. Jones, T. R., Webber, S. E., Varney, M. D., Reddy, M. R., Lewis, K. K., Kathardekar, V., Mazdiyasni, H., Deal, J., Nguyen, D., Welsh, K. M., Webber, S., Johnston, A., Matthews, D. A., Smith, W. W., Janson, C. A., Bacquet, R. J., Howland, E. F., Booth, C. L., Herrmann, S. M., Ward, R. W., White, J., Bartlett, C. A., and Morse, C. A. (1997) *J. Med. Chem*. **40,** 677–683
11. Bolin, T. J., Filman, D. J., Matthews, D. A., Hamlin, R. C., and Kraut, J. (1982) *J. Biol. Chem.* **257,** 13650–13662
12. Reich, S. H., Fuhry, M. A., Nguyen, D., Pino, M. J., Welsh, K. M., Webber, S., Janson, C. A., Jordan, S. R., Matthews, D. A., Smith, W. W., Bartlett, C. A., Booth, C. L. J., Herrmann, S. M., Howland, E. F., Morse, C. A., Ward, R. W., and White, J. (1992) *J. Med. Chem.* **35,** 847–858
13. Waheed, A. A., Rao, S. K., and Gupta, P. D. (2000) *Anal. Biochem.* **287,** 73–79
14. McGovern, S. L., Caselli, E., Grigorieff, N., and Shoichet, B. K. (2002) *J. Med. Chem.* **45,** 1712–1722
15. Shoichet B. K., Bodian D. L., and Kuntz, I. D. (1992) *J. Comput. Chem.* **13,** 380–397
16. Meng, E. C., Shoichet, B. K., and Kuntz, I. D. (1992) *Comput. Chem.* **13,** 505–524
17. Shoichet, B. K., and Kuntz, I. D. (1993) *Protein Eng.* **6,** 723–732
18. Gilson, M. K., and Honig, B. (1991) *J. Comput. Aided Mol. Des.* **5,** 5–20
19. Rashin, A. A. (1990) *J. Phys. Chem.* **94***,* 1725–1733
20. Gilson, M. K., and Honig, B. H. (1987) *Nature* **330,** 84–86

21. Guner, O. F., Hughes, D. W., and Dumont, L. M. (1991) *J. Chem. Inf. Comput. Sci.* **31,** 408–414
22. Gasteiger J., and Marsili, M. (1980) *Tetrahedron* **36,** 3219–3288
23. Meng, E. C., Gschwend, D. A., Blaney, J. M., and Kuntz, I. D. (1993) *Proteins* **17,** 266–278
24. Ferrin, T. E., Huang, C. C., Jarvis, L. E., and Langridge, R. (1988) *J. Mol. Graph.* **6,** 13–27, 36–37
25. Blakley, R. L. (1960) *Nature* **188,** 231–232
26. Grumont, R., Sirawaraporn, W., and Santi, D. V. (1988) *Biochemistry* **27,** 3776–3784
27. Meek, T. D., Garvey, E. P., and Santi, D. V. (1985) *Biochem.* **24,** 678–686
28. Grumont, R., Washtein, W. L., Caput, D., and Santi, D. V. (1986) *Proc. Natl. Acad. Sci. U. S. A.* **83,** 5387–5391
29. Roos, D. S., Donald, R. G. K., Morissette, N. S., and Moulton, A. L. C. (1994) *Methods Cell Biol.* **45,** 27–63
30. Nakaar, V., Samuel, B. U., Ngo, E. O., and Joiner, K. A. (1999) *J. Biol. Chem.* **274,** 5083–5087
31. Li, J. B., Zhu, T. H., Cramer, C. J., and Truhlar, D. G. (1998) *J. Phys. Chem.* **102,** 1820–1831
32. Anderson, K. S. (1999) *Methods Enzymol.* **308,** 111–145
33. Anderson, K. S., and Johnson, K. A. (1990) *Chem. Rev.* **90,** 1131–1149
34. Schwab, J. C., Beckers, C. J. M., and Joiner, K. A. (1994) *Proc. Natl. Acad. Sci. U. S. A.* **91,** 509–513
35. Desai, S. A., and Rosenberg, R. L. (1997) *Proc. Natl. Acad. Sci. U. S. A.* **94,** 2045–2049
36. Schneider G., and Bohm, H. J. (2002) *Drug Discov. Today* **7,** 64–70
37. Tondi, D., Powers, R. A., Caselli, E., Negri, M. C., Blazquez, J., Costi, M. P., and Shoichet, B. K. (2001) *Chem. Biol.* **8,** 593–611